

Arbitrary scaling of images using an M-channel DFT filter bank with optimized adaptive interpolation kernels

J. Y. Kim and S. W. Nam^{a)}

Department of Electronics and Computer Engineering, Hanyang University,
Seoul, 133–791, Korea

a) swnam@hanyang.ac.kr

Abstract: A new approach to arbitrary scaling of high quality images is proposed, whereby a 2-D M-channel DFT filter bank is designed along with its synthesis part being modified on the basis of a compactly supported sampling function. For that purpose, the 2-D down/up-sampling formulae in a closed form are derived and utilized. Also, an optimized adaptive interpolation technique is employed to compensate for quality degradation arising in scaled images. Finally, simulation results demonstrate that high quality images of arbitrary size can be obtained from the original image.

Keywords: arbitrary scalability, M-ch DFT filter bank, compactly supported sampling function (CSSF), optimized adaptive interpolation

Classification: Science and engineering for electronics

References

- [1] G. Pau, B. P.-Popescu, and G. Piella, “Modified M-band synthesis filter bank for fractional scalability of images,” *IEEE Signal Process. Lett.*, vol. 13, no. 6, June 2006.
- [2] F. Itami, E. Watanabe, and A. Nishihara, “A new multirate processing scheme for the conversions of image resolution based on integer/fractional sampling filter banks,” *IEICE Technical Report*, vol. 105, no. 149, SIP2005-34, pp. 55–60, June 2005.
- [3] S. C. Pei and M. P. Kao, “Two channel nonuniform perfect reconstruction filter bank with irrational down-sampling factors,” *IEEE Signal Process. Lett.*, vol. 12, no. 2, pp. 116–119, Feb. 2005.
- [4] E. H. W. Meijering, K. J. Zuiderveld, and M. A. Viergever, “Image reconstruction by convolution with symmetrical piecewise nth-order polynomial kernels,” *IEEE Trans. Image Process.*, vol. 8, no. 2, pp. 192–201, Feb. 1999.
- [5] A. Fujii, K. Kameyama, T. Kamina, Y. Ohmiya, and K. Toraiichi, “Image resolution conversion by optimized adaptation of interpolation kernels,” *Proc. 24th IASTED Int. Multi-Conf. on Signal Processing, Pattern Recognition, and Applications*, pp. 274–279, 2006.
- [6] G. Strang and T. Nguyen, *Wavelets and Filter Banks*, Wellesley-

Cambridge Press, Massachusetts, Wellesley, 1996.

1 Introduction

Today, digital images and video frames can be transmitted over networks and displayed in various multimedia devices. Accordingly, image reconstruction with a wide range of scalability has become an important issue. Recently, digital filter banks have found many applications in image processing and digital communication (e.g., subband coding and signal transmission). In particular, a dyadic scalability can be achieved by using the wavelet transform based subband coding. Furthermore, such dyadic wavelets can be extended to M-band wavelets to obtain finer scalability, yielding M-band filter banks. Also, some filter bank structures with arbitrary rational scalability were proposed [1, 2]. However, those filter bank approaches require that both analysis and synthesis filters, satisfying reconstruction conditions, should be redesigned each time a different rational scaling factor is required. For example, the number of channels in the analysis part of the filter bank should be changed, depending on the required rational scaling factors. Moreover, compensation for quality degradation arising in reconstructed images has not been incorporated into the filter bank structure.

In this paper, a new 2-D M-channel DFT filter bank with a modified synthesis part is proposed for arbitrary scaling of images, whereby 2-D closed-form down/up-sampling formulae based on a compactly supported sampling function (CSSF) are utilized. Also, an optimized adaptive interpolation (OAI) technique is employed to compensate for quality degradation of reconstructed images.

2 Closed-form down/up sampling formulae using a CSSF

In [3], a perfect reconstruction (PR) filter bank was reported for arbitrary sampling rate conversion in a single step, whereby down/up-sampling formulae in a closed form were introduced by employing a sinc function as an ideal interpolation kernel. However, there is a practical difficulty in utilizing the sinc function (e.g., due to its infinite support or truncation effect) [4]. Recently, the following interpolation kernel of finite length (called CSSF of degree 2 : $\psi_{[s],0}^3(t)$) was introduced from the fluency theorems [5]:

$$\psi_{[s],0}^3(t) = -\frac{1}{2}\phi_3(t+2) + 2\phi_3\left(t + \frac{3}{2}\right) - \frac{1}{2}\phi_3(t+1) \quad (1)$$

$$\phi_1(t) = \begin{cases} 1, & 0 \leq t \leq 1 \\ 0, & \text{otherwise} \end{cases}, \quad \phi_3(t) = \phi_1(t) * \phi_1(t) * \phi_1(t) \quad (2)$$

In (1)–(2), $\phi_3(t)$ is a piecewise polynomial of degree 2, calculated by double convolutions with $\phi_1(t)$, and $\psi_{[s],0}^3(t)$ is of finite support, thus suitable for high speed image processing. By utilizing the CSSF of degree 2 as a sampling kernel, i.e., by replacing the sinc function of the down/up sampling formulae

in [3] by $\psi_{[s],0}^3(t)$, we can obtain the following modified down/up sampling formulae:

$$x_{\downarrow M}(n) = \frac{1}{M} \sum_k x(k) \psi_{[s],0}^3 \left(n - \frac{k}{M} \right),$$

$$M \cdot (n - 2) < k < M \cdot (n + 2), \quad k \neq M \cdot (n \pm 1) \quad (3)$$

$$x_{\uparrow M}(n) = \sum_k x(k) \psi_{[s],0}^3 \left(\frac{n}{M} - k \right), \quad \frac{n}{M} - 2 < k < \frac{n}{M} + 2, \quad k \neq \frac{n}{M} \pm 1$$

$$(4)$$

3 An optimized adaptive interpolation (OAI) technique

In this paper, the optimized adaptive interpolation technique (OAI) in [5] is also employed to compensate for image quality degradation, due to edge blur and jagged noise, arising in reconstructed images. More specifically, the shapes of up-sampling kernels are adaptively deformed, depending on the direction of the edges, for the control of the influence of the sampling pixels near edges of the original images. For that purpose, the concept of an expansion/contraction rate in the direction of the axis connecting the sampling and reconstructed pixels is utilized along with optimal parameters (e.g., E_{\max} , R_{\max} , L , V_s) estimated by the particle swarm optimization (PSO) [5] to obtain a scaled image with higher PSNR.

4 The proposed 2-D M-ch DFT Filter bank scheme

The DFT filter bank structure has several advantages (e.g., design simplicity and high speed implementation), since it can be designed on the basis of a prototype low-pass filter along with complex modulation. However, it is known that the DFT filter bank structure may not go well with perfect reconstruction (PR) [6]. On the other hand, design of analysis and synthesis filters in an M-ch PR filter bank is very restrictive when $M > 2$, due to the PR conditions. To solve these problems, the following down/up-sampling kernels modified with an expansion/contraction rate are introduced to compensate for quality degradation in reconstructed images:

$$\psi_{[s],0}^3(n, k)_{\downarrow M} = \psi_{[s],0}^3 \left(\left(n - \frac{k}{M} \right) / \gamma_D \right) \quad (5)$$

$$\psi_{[s],0}^3(n, k)_{\uparrow M} = \psi_{[s],0}^3 \left(\left(\frac{n}{M} - k \right) / \gamma_D \right) \quad (6)$$

In (5)–(6), the expansion/contraction rate (γ_D), provided by the OAI process [5], is used in the modified synthesis part of the proposed filter bank of Fig. 1: $G(x, y)$ is the gray level at the pixel (x, y) of the original image, $S(x, y)$ is the gray level at pixel (x, y) of the scaled image, W_M is defined as $e^{-j2\pi/M}$, and the OAI technique [5] is utilized. In particular, down/up-samplers with pre-/post-filters in a conventional M-ch filter bank are replaced by the horizontal and vertical blocks corresponding to 2-D extension of (3)–(4), as described in Fig. 1 and Table I. Also, the matrix-form input-output relationship of each block is included in Table I. More specifically, in the

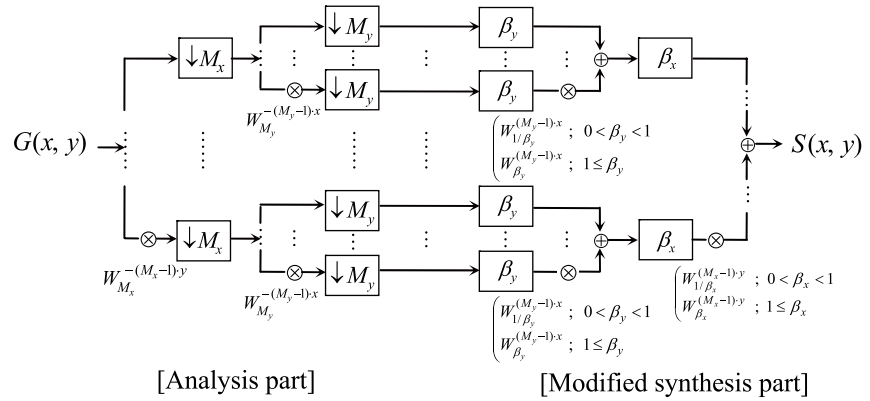


Fig. 1. The 2-D M-ch DFT filter bank scheme with a modified synthesis part

analysis part, each row of an input image is down-sampled in the horizontal direction by $1/M_x$, by applying the 2-D closed-form down-sampling formula (i.e., $H_{\downarrow M_x}$). Also, each column of the input image is down-sampled in the vertical direction by $1/M_y$, by applying the 2-D closed-form down-sampling formula (i.e., $H_{\downarrow M_y}$). In the modified synthesis part, 2-D closed-form formulae and matrix-form input-output relationship of each block are also provided, where the expansion/contraction rate parameter γ_D is incorporated into the 2-D closed-form formulae. In addition, β_x (or β_y) in the modified synthesis part can be determined by multiplying M_x (or M_y) by desired scaling factors (e.g., α_x (or α_y)) in the horizontal (or vertical) direction: i.e.,

$$\beta_x = M_x \times \alpha_x, \quad \beta_y = M_y \times \alpha_y \quad (7)$$

In (7), M_x and M_y correspond to the numbers of channels in horizontal and vertical directions, respectively. When $0 < \beta_x, \beta_y < 1$, the 2-D down-sampling formulae (i.e., $H_{\downarrow 1/\beta_x}$, $H_{\downarrow 1/\beta_y}$) are applied to the input image. On the other hand, when $1 \leq \beta_x, \beta_y$, the 2-D up-sampling formulae (i.e., $H_{\uparrow \beta_x}$, $H_{\uparrow \beta_y}$) can be applied to the input image. Moreover, the modified 2-D down/up-sampling kernels as in Table I (i.e., (5)–(6)) can be utilized for the pixels near edges of a subband image, along with the OAI technique with the expansion/contraction rate γ_D to improve the reconstructed image quality. Note that, for the pixels far from the edges of the given image, (5)–(6) with $\gamma_D = 1$ can be applied. In this way, arbitrary scaled images of high quality along the vertical (and/or horizontal) direction can be obtained from the original image, directly without post-resampling and without changing the number of channels in the analysis part, by applying the proposed approach.

5 Simulation results

To verify the performance of the proposed approach, the four images as in Fig. 2 (b)–Fig. 2 (e), reconstructed from the original 8-bit gray scale ‘Lena’ image of 256×256 size, are obtained by applying the proposed 2-ch filter bank along each direction, where the desired scaling factors, α_x ($= \alpha_y$), are given by $2/3$, $8/9$, 1 , and $4/3$, respectively. Also, optimal parameters for the

Table I. 2-D closed-form down/up-sampling formulae and matrix representations for the input-output relationship of each block

Parts	Directions	Blocks	closed-form and matrix-form representation for the input($g(x,y)$) - output($f(x,y)$) relationship of each block
Analysis	Horizontal	\downarrow_{M_x}	$f_{\downarrow_{M_x}}(x,y) = \frac{1}{M_x} \sum_{(k,l)} g(k,l) \psi_{[s],0}^3(x-k) \psi_{[s],0}^3(y - \frac{l}{M_x})$ <p>where $(x-2, M_x \cdot (y-2)) < (k,l) < (x+2, M_x \cdot (y+2))$, $(k,l) \neq (x \pm 1, M_x \cdot (y \pm 1))$</p>
			$G \cdot H_{\downarrow_{M_x}} = F, \quad G \in \mathfrak{R}^{P \times Q}, \quad H_{\downarrow_{M_x}} \in \mathfrak{R}^{Q \times [Q/M_x]}$ $H_{\downarrow_{M_x}} = [h_{ij}], \quad \text{where } h_{ij} = \frac{1}{M_x} \cdot \psi_{[s],0}^3(j - \frac{i}{M_x})$
Analysis	Vertical	\downarrow_{M_y}	$f_{\downarrow_{M_y}}(x,y) = \frac{1}{M_y} \sum_{(k,l)} g(k,l) \psi_{[s],0}^3(x - \frac{k}{M_y}) \psi_{[s],0}^3(y-l)$ <p>where $(M_y \cdot (x-2), y-2) < (k,l) < (M_y \cdot (x+2), y+2)$, $(k,l) \neq (M_y \cdot (x \pm 1), y \pm 1)$</p>
			$H_{\downarrow_{M_y}} \cdot G = F, \quad G \in \mathfrak{R}^{P \times Q}, \quad H_{\downarrow_{M_y}} \in \mathfrak{R}^{[P/M_y] \times P}$ $H_{\downarrow_{M_y}} = [h_{ij}], \quad \text{where } h_{ij} = \frac{1}{M_y} \cdot \psi_{[s],0}^3(i - \frac{j}{M_y})$
Modified Synthesis	Horizontal	β_x	$f_{\downarrow_{\beta_x}}(x,y) = \beta_x \cdot \sum_{(k,l)} g(k,l) \psi_{[s],0}^3(x-k) \psi_{[s],0}^3((y - \beta_x \cdot l) / \gamma_D)$ <p>where $(x-2, 1/\beta_x \cdot (y-2 \cdot \gamma_D)) < (k,l) < (x+2, 1/\beta_x \cdot (y+2 \cdot \gamma_D))$, $(k,l) \neq (x \pm 1, 1/\beta_x \cdot (y \pm \gamma_D))$</p>
			$G \cdot H_{\downarrow_{\beta_x}} = F, \quad G \in \mathfrak{R}^{P \times Q}, \quad H_{\downarrow_{\beta_x}} \in \mathfrak{R}^{Q \times [Q/\beta_x]}$ $H_{\downarrow_{\beta_x}} = [h_{ij}], \quad \text{where } h_{ij} = \beta_x \cdot \psi_{[s],0}^3((j - \beta_x \cdot i) / \gamma_D)$
	Vertical	β_y	$f_{\uparrow_{\beta_y}}(x,y) = \sum_{(k,l)} g(k,l) \psi_{[s],0}^3(x-k) \psi_{[s],0}^3(\frac{y-l}{\beta_y} / \gamma_D)$ <p>where $(x-2, -2 \cdot \gamma_D + y / \beta_x) < (k,l) < (x+2, 2 \cdot \gamma_D + y / \beta_x)$, $(k,l) \neq (x \pm 1, y / \beta_x \pm \gamma_D)$</p>
			$G \cdot H_{\uparrow_{\beta_y}} = F, \quad G \in \mathfrak{R}^{P \times Q}, \quad H_{\uparrow_{\beta_y}} \in \mathfrak{R}^{Q \times [Q/\beta_y]}$ $H_{\uparrow_{\beta_y}} = [h_{ij}], \quad \text{where } h_{ij} = \psi_{[s],0}^3(\frac{j}{\beta_y} - i) / \gamma_D$
Modified Synthesis	Horizontal	β_x	$f_{\downarrow_{\beta_x}}(x,y) = \beta_x \cdot \sum_{(k,l)} g(k,l) \psi_{[s],0}^3((x - \beta_x \cdot k) / \gamma_D) \psi_{[s],0}^3(y-l)$ <p>where $(1/\beta_x \cdot (x-2 \cdot \gamma_D), y-2) < (k,l) < (1/\beta_x \cdot (x+2 \cdot \gamma_D), y+2)$, $(k,l) \neq (1/\beta_x \cdot (x \pm \gamma_D), y \pm 1)$</p>
			$H_{\downarrow_{\beta_x}} \cdot G = F, \quad G \in \mathfrak{R}^{P \times Q}, \quad H_{\downarrow_{\beta_x}} \in \mathfrak{R}^{[P/\beta_x] \times P}$ $H_{\downarrow_{\beta_x}} = [h_{ij}], \quad \text{where } h_{ij} = \beta_x \cdot \psi_{[s],0}^3((i - \beta_x \cdot j) / \gamma_D)$
Modified Synthesis	Vertical	β_y	$f_{\uparrow_{\beta_y}}(x,y) = \sum_{(k,l)} g(k,l) \psi_{[s],0}^3(\frac{x-k}{\beta_y} / \gamma_D) \psi_{[s],0}^3(y-l)$ <p>where $(-2 \cdot \gamma_D + x / \beta_y, y-2) < (k,l) < (2 \cdot \gamma_D + x / \beta_y, y+2)$, $(k,l) \neq (x / \beta_y \pm \gamma_D, y \pm 1)$</p>
			$H_{\uparrow_{\beta_y}} \cdot G = F, \quad G \in \mathfrak{R}^{P \times Q}, \quad H_{\uparrow_{\beta_y}} \in \mathfrak{R}^{[P/\beta_y] \times P}$ $H_{\uparrow_{\beta_y}} = [h_{ij}], \quad \text{where } h_{ij} = \psi_{[s],0}^3(\frac{i}{\beta_y} - j) / \gamma_D$

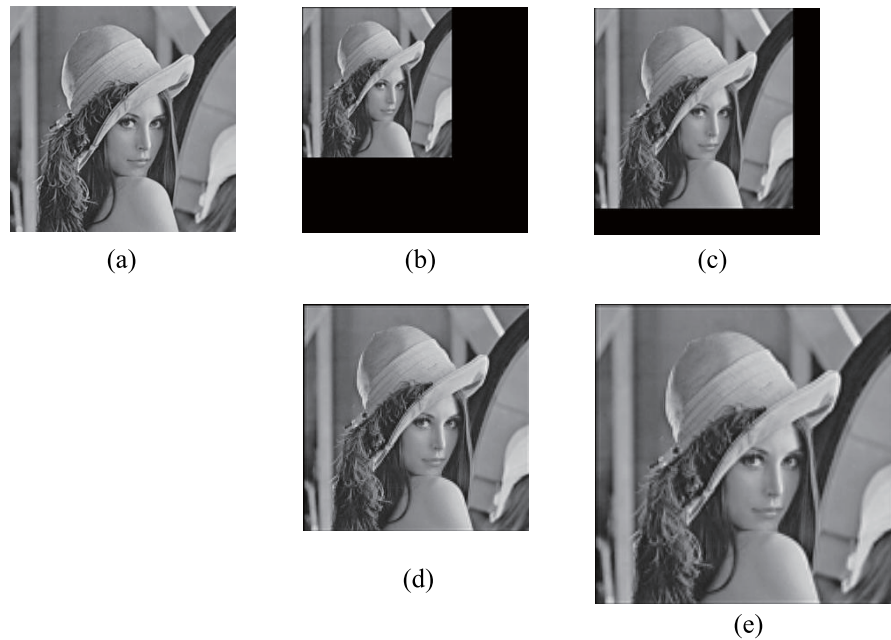


Fig. 2. (a) The original ‘Lena’ image and the reconstructed images with desired scaling factors of (b) 2/3, (c) 8/9, (d) 1, and (e) 4/3 in each direction

OAI technique, estimated by applying the PSO method 100 times, are given by

$$E_{\max} = -0.0146, \quad R_{\max} = -0.0802, \quad L = 1, \quad V_s = 595.3402 \quad (8)$$

Figure 2(b)–(e) show that all four scaled ‘Lena’ images with scaling factors (2/3, 8/9, 1, and 4/3), reconstructed from the original image (i.e., Fig. 2(a)), are of high quality. In addition, the ‘Lena’ image of 64×64 size is also used in the PSO procedure for a simple performance comparison in case of $\alpha_x = \alpha_y = 1$ (i.e., between Fig. 2(a) and Fig. 2(d)). More specifically, the image reconstructed with scaling factor 1 (i.e., Fig. 2(d)), obtained by the proposed approach with the OAI technique, yields high image quality (i.e., PSNR = 31.77 dB). Note that the image obtained by the proposed approach without the OAI technique results in 31.55 dB PSNR. Accordingly, we can see that high quality images of arbitrary size can be obtained by applying the proposed filter bank scheme with an OAI technique.

6 Conclusion

In this paper, a new filter-bank based approach to arbitrary scaling of high quality images is presented. For that purpose, a 2-D M-channel DFT filter bank with its synthesis part being modified on the basis of a CSSF of degree 2 is utilized along with an optimized adaptive interpolation technique. The performance of the proposed approach is demonstrated by showing that high quality images of arbitrary size can be obtained. Our future work includes further development of the proposed approach by employing a non-separable 2-D filter bank and a modulated filter bank structure with PR property.

Acknowledgments

This study was supported by a grant of the Korea Health 21 R & D Project, Ministry of Health & Welfare, and Republic of Korea (02-PJ3-PG6-EV08-0001).